Journal of Power Sources 249 (2014) 435–439

Contents lists available at ScienceDirect

Journal of Power Sources

journal homepage: www.elsevier.com/locate/jpowsour

Short communication

Effect of temperature on the performances and in situ polarization analysis of zinc–nickel single flow batteries

Yuanhui Cheng [a,b], Huamin Zhang [a,*], Qinzhi Lai [a,**], Xianfeng Li [a], Qiong Zheng [a], Xiaoli Xi [a,b], Cong Ding [a,b]

[a] Division of Energy Storage, Dalian Institute of Chemical Physics, Chinese Academy of Sciences, Dalian 116023, PR China
[b] University of Chinese Academy of Sciences, Beijing 100039, PR China

HIGHLIGHTS

- ZNBs can operate in the temperature of 0 °C–40 °C with acceptable efficiency.
- The temperature sensitivity of CE and EE are 0.65% °C^{-1} and 0.98% °C^{-1}.
- The positive polarization is a major obstacle to enhance the VE.
- The proton transfer in positive electrode is more sensitive to temperature.

ARTICLE INFO

Article history:
Received 25 September 2013
Received in revised form
22 October 2013
Accepted 24 October 2013
Available online 5 November 2013

Keywords:
Batteries
Energy storage
Zinc–nickel
Temperature effect
Polarization distribution

ABSTRACT

The recently proposed high power density zinc–nickel single flow batteries (ZNBs) exhibit great potential for larger scale energy storage. The urgent needs are in the research into temperature adaptability of ZNBs before practical utilization. Furthermore, making clear their polarization distribution is essential to direct the further improvement of battery performance. Here, we focus on the trends in the polarization distribution and effect of temperature on the performance of ZNBs. The result shows that ZNBs can operate in the temperature range from 0 °C to 40 °C with acceptable energy efficiency (53%–79.1%) at 80 mA cm^{-2}. The temperature sensitivity of coulombic efficiency and energy efficiency are 0.65% °C^{-1} and 0.98% °C^{-1} at 0 °C–20 °C, respectively. The positive polarization is much larger than the negative polarization at all studied temperatures. The charge overpotential of the positive electrode is more sensitive to temperature. These results enable us to better evaluate the application prospect of ZNBs and point a clear struggling orientation to further improve the battery performance.

1. Introduction

To further utilize the excess power generation and intermittent renewable energy resources, the development of large capacity, low cost, highly efficient and safe energy storage devices is the most urgent demand. Flow batteries (FBs) are very appealing storage devices for these requirements [1,2]. However, expensive membranes hinder their large scale application. Various attempts have been made to reduce the integration cost [3–12]. Eliminating membranes without compromising performance opens up new ways to address this challenge. Zinc–nickel single flow batteries (ZNBs) along with naturally plenty and non-toxic raw materials of zinc and nickel, exhibit an attractive application prospect. However, ZNBs have been operated at the current density below 20 mA cm^{-2} due to the large polarization resistance, resulting in a low power density [13,14]. Recently, we have improved the current density by as much as four times approaching 80 mA cm^{-2} without seriously compromising the storage efficiency through designing novel cell structures [15]. Then, the storage efficiency is further boosted by introducing three-dimensional porous electrodes to ZNBs to decrease the polarization of the negative electrode [16]. Such, this system with excellent performance is on the way to realize commercial application for energy storage.

However, these energy storage devices are usually used in different climate areas (typically 0 °C–40 °C). It is well known that the temperature can affect the properties of electrolyte and electrode kinetics pronouncedly, which thereby influences the battery performance [2,17–19]. In the case of the vanadium flow battery, temperature plays a significant role in its performances of battery and electrode due to the stability and solubility of vanadium ion

* Corresponding author. Tel.: +86 411 84379072; fax: +86 411 84665057.
** Corresponding author. Tel.: +86 411 84379669; fax: +86 411 84665057.
E-mail addresses: zhanghm@dicp.ac.cn (H. Zhang), qinzhilai@dicp.ac.cn (Q. Lai).

0378-7753/$ – see front matter © 2013 Elsevier B.V. All rights reserved.
http://dx.doi.org/10.1016/j.jpowsour.2013.10.115

species. The precipitation of V (V) ions at temperature above 40 °C, and V (III) and V (II) ions at temperature below 10 °C, especially at the high concentration above 2 mol L^{-1}, make VFB only operated in a narrow temperature range of 10 °C–40 °C [17,18]. As to the soluble lead acid flow battery, forming the rough or powdery deposits at a higher temperature will lead to the shedding of lead dioxide into solution and thus bring about the charge imbalance. As a result, the soluble lead acid flow battery should be operated closely to room temperature [19]. The operating temperature of the polysulphide-bromine battery is typically between 20 °C and 40 °C [2]. However, currently, no works about the influence of temperature on the performance of ZNBs have been reported. Temperature will affect electrode reaction kinetics (proton diffusion and formation of zinc nuclei), electrolyte properties and chemical dissolution of zinc. Furthermore, the parasitic reaction rates of oxygen evolution at the positive electrode and hydrogen evolution at the negative electrode mainly depend on the temperature. Therefore, it is of great value to investigate the effect of temperature on battery performance before practical application.

Besides, in order to further optimize the battery performance, the polarization (activation, ohmic and concentration) must be still minimized to achieve excellent efficiency. Since the electrode polarization containing both activation and concentration polarizations, is the key factor in determining final battery performance, the optimization of electrode becomes an effective way to improve battery performance. Accordingly, the in situ electrode polarization distribution between negative and positive electrodes is needed for definitive validation. These features are used to evaluate and predict potential problems arising during battery operation and to direct the optimization of electrode polarization. Here, electrode properties, battery performances and polarization distributions under various temperatures (0 °C–40 °C) were investigated in detail.

2. Experimental section

2.1. Chemicals

Analytical zinc oxide and potassium hydroxide were used without further treatment. An aqueous solution of 0.4 mol dm^{-3} potassium zincate mixed with 8 mol dm^{-3} potassium hydroxide was used as electrolyte, made by dissolving zinc oxide in potassium hydroxide aqueous solution. The prepared electrolyte was colorless without precipitation.

2.2. Electrochemical measurements

CHI 612C potentiostat (Shanghai Chenhua Instrumental Co., Ltd., China) was used to conduct electrochemical experiments in a traditional three-electrode glass cell. For the half cell of negative reaction, the working electrode was a piece of nickel foams (2 mm × 5 mm × 2 mm, 110 PPI, 420 g m^{-2}, Changsha Lyrun Material Co., Ltd., China). The counter electrode was sintered nickel hydroxide (20 mm × 30 mm × 0.7 mm, Jiangsu Highstar Battery Manufacturing, China). An Hg/HgO electrode (0.98 V vs. the standard hydrogen electrode (SHE)) was used as reference electrode. For the half cell of positive reaction, a sintered nickel hydroxide (3 mm × 5 mm × 0.7 mm) was used as the working electrode, while a piece of graphite (20 mm × 30 mm × 1.7 mm) as the counter electrode, and an Hg/HgO electrode as the reference electrode. These half cells were settled in a constant temperature oven (Wuxi Boleda Experimental Equipment Co., Ltd., China) to maintain the temperature at a certain value in the range of 0 °C–40 °C. The cyclic voltammetry was measured in the same potential window at a scan rate of 20 mV s^{-1} for both negative and positive half cells. After measurement, all potentials were revised to SHE, which is assumed to be independent of temperature [20]. The current density was normalized to the geometrical area of working electrodes.

2.3. Single cell measurements

The electrical and electrolytic circuits of the flow battery are shown in Fig. 1. The positive electrode was nickel hydroxide electrode (30 mm × 30 mm × 0.7 mm) with a capacitor of 25 mAh cm^{-2}. The negative electrode was nickel foam (30 mm × 30 mm × 2 mm). The distance of the two electrodes was 5 mm. An aqueous solution of 8 mol dm^{-3} potassium hydroxide mixed with 0.4 mol dm^{-3} zinc oxide was used as electrolyte circulated by a pump. The cell was charged and discharged under the same constant current density (80 mA cm^{-2}) conducted by Arbin BT-2000. The battery was charged to 80% capacitance based on the positive electrode and discharged to 0.8 V. The positive and negative potentials were continuously monitored on one completed cycle by setting an Hg/HgO reference electrode in the middle of the gap between two electrodes. This single cell was measured at the temperature of 0 °C–40 °C controlled in a constant temperature oven.

3. Results and discussion

3.1. Electrochemical performance

The reactivity and reversibility are two key indexes to calculate electrochemical performances of the electrode reactions. The electrochemical reactions of positive and negative electrodes at various temperatures (0 °C–40 °C) were tested using cyclic voltammetry at 20 mV s^{-1} in the same potential width (Fig. 2). Potential is revised to the standard hydrogen electrode (SHE). Their reactivity and reversibility increase along with the increasing temperature. The reactivity and reversibility of positive electrode reaction ($Ni(OH)_2 + OH^- = NiOOH + e$) are lower than that of negative electrode reaction ($[Zn(OH)_4]^{2-} + 2e = Zn + 4OH^-$). With the temperature increasing from 0 °C to 40 °C, the peak current density of Zn oxidation increases 1.9 times, while the peak reduction current of NiOOH enhances 2.5 times. The positive electrode reaction seems to be more sensitive to temperature than the

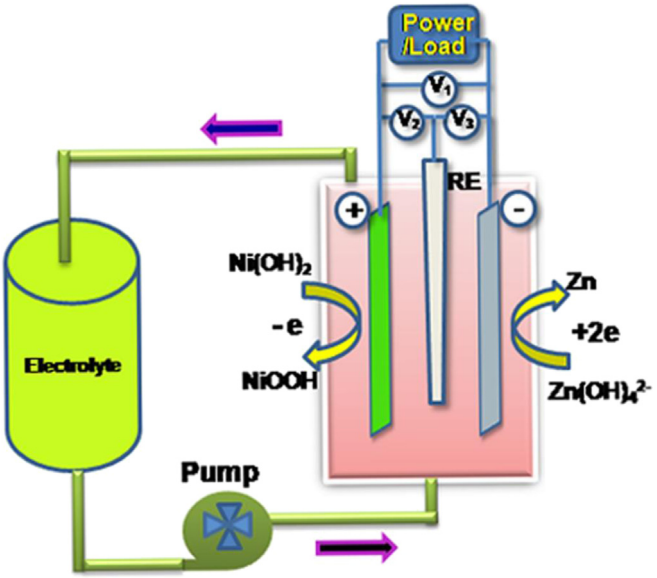

Fig. 1. Electrical and electrolytic circuits of ZNBs.

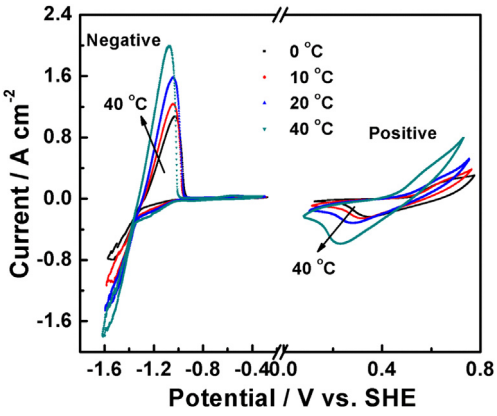

Fig. 2. A combined cyclic voltammetry of zinc half-cell and nickel half-cell reactions at 20 mV s^{-1}.

negative electrode reaction. Besides, it is difficult to eliminate the parasitic reactions, hydrogen and oxygen evolution due to the close accompany with the main reactions. The output voltage and charge voltage could be sketchily estimated by subtracting negative electrode potential from positive electrode potential. With the increasing temperature, the output voltage increases, while the charge voltage decreases, which lead to higher voltage efficiency (VE). The above results show that the positive electrode reaction is the critical obstacle for the reduction of full-cell polarization. Highly active nickel hydroxide electrodes can effectively lower large polarization resistance of positive electrodes, which hinder the improvement of the battery performance.

3.2. Voltage characteristics

The charge–discharge voltage curves at various temperatures are expressed in Fig. 3. Generally, the curve shows a relatively flat cell voltage. With the temperature increasing from 0 °C to 40 °C, the charge voltage decreases, while the discharge voltage increases, due to the enhanced conductivity of electrolytes and reactivity of electrode reactions. As a result, a high VE was obtained at higher temperature because of the lower polarization resistance. A quick increase of charge voltage appears at the beginning of charging process at 0 °C, while others increase gradually. This is due to the slow formation rate of zinc nuclei at the negative electrode or the slow transfer rate of proton at the positive electrode.

The mid-voltage is one critical indicator of the charge voltage and output voltage. The mid-voltages as a function of temperature during the charging and discharging process are shown in Fig. 4. With the increasing temperature, the mid-charge voltage decreases, while the mid-discharge voltage increases. Compared to 0 °C, the mid-charge voltage decreases 280 mV, while the mid-discharge voltage increases 163 mV at 40 °C. The polarization resistance decreases distinctly. Therefore, a higher output voltage and a higher VE can be realized at higher temperature. Distinguishing the polarization distribution between negative and positive electrodes is needed for the intensive improvement of battery performance.

3.3. Battery performance

Since battery may be used at various temperatures, especially from 0 °C to 40 °C, it is of great importance to investigate the rapid start-up properties and efficiencies at different temperatures before its practical applications in grid energy storage and renewable integration (Fig. 5). The coulombic efficiency (CE), which is defined as the ratio of a cell's discharge capacity to its charge capacity, increase dramatically from 80.7% to 96.3% along with the temperature range from 0 °C to 40 °C. This tendency might be ascribed to the little electric charge for side reaction and capacitance that result from lower charge voltage. Meanwhile, the voltage efficiency (VE), which is determined by the ratio of a cell's mean discharge voltage divided by its mean charge voltage, increases along with the temperature. This result can be explained by the lower polarization on both positive and negative electrodes, which are decided by reactivity of main electrode reactions and electrolyte properties at high temperatures. Accordingly, the energy efficiency (EE), which is one of the most important parameters, increases dramatically from 53% to 79.1% with the increasing temperature. A linear relationship is observed in the range of 0 °C–20 °C. The temperature sensitivity of CE and EE are 0.65% $°C^{-1}$ and 0.98% $°C^{-1}$, respectively. A deviation is observed from 20 °C to 40 °C. The effect of temperature on battery performance in the range of 20 °C–40 °C is smaller compared to lower temperature. The above results confirm that the temperature plays a significant role in the battery performance. Overall, unlike other battery systems, no obstacle was observed in starting up the battery in all case. ZNBs can operate in the temperature range from 0 °C to 40 °C with acceptable energy efficiency.

3.4. Polarization analysis

In order to determine the polarization distribution between two electrodes, the half-cell potentials were measured by in situ monitoring the negative electrode potential and the positive

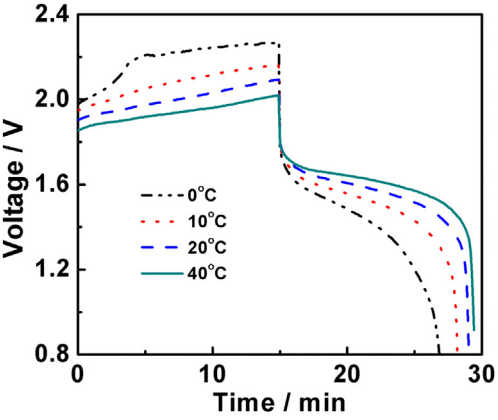

Fig. 3. Charge–discharge voltage curves under various temperatures.

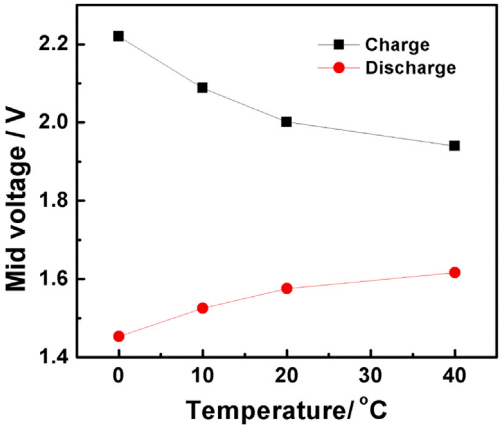

Fig. 4. Mid-charge and mid-discharge voltages under various temperatures.

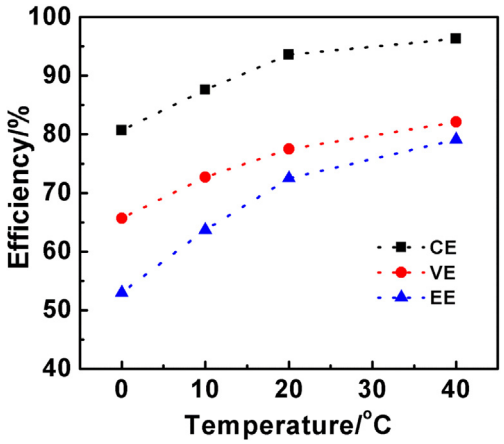

Fig. 5. Coulombic efficiency (CE), voltage efficiency (VE) and energy efficiency (EE) under various temperatures.

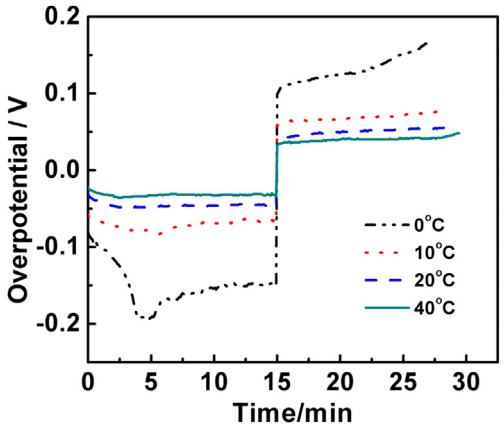

Fig. 7. Overpotential of negative electrode under various temperatures.

electrode potential during the charging and discharging process at various temperatures (0 °C–40 °C). Evidently, the overpotentials of the positive electrode and negative electrode both decrease along with the increasing temperature (Figs. 6 and 7). With the temperature increasing, the reduction of polarization can be mainly attributed to the lower electrochemical polarization and ohmic polarization, which is in good agreement with the results of charge/discharge potentials and voltage efficiencies. A rapidly and linearly increase of negative overpotential only presents at 0 °C in Fig. 7. This is due to the higher formation energy of zinc nuclei at low temperature. Following the hydrogen evolution current, the current of zinc deposition increases exponentially, suggesting progressive nucleation. The time, reaching maximum overpotential, shows how long it takes nuclei to fully overlap one another and completely cover the electrode surface [21]. The overpotential of the positive electrode is much larger than that of the negative electrode, which is consistent with the cyclic voltammograms at various temperatures.

The mid-overpotentials during the charging and discharging process have the same tendency as overpotentials as exhibited in Fig. 8. With the temperature increasing from 0 °C to 40 °C, the mid-overpotential ratio of the positive electrode to the negative electrode increases from 2.1 to 4.4 during the charging process, while this ratio increases from 1.8 to 3 during the discharging process. The mid-overpotentials of the positive electrode are much larger than that of the negative electrode during the charging and discharging process, which is a main obstacle to enhance the VE. This is due to low activity of nickel hydroxide electrode caused by the sluggish transfer of proton [22,23].

The mid-overpotentials of the negative electrode during the charging and discharging process are approximately equal (except for 0 °C) resulting from the equal reactivity of the reduced and oxidized reactions. The slow deposition rate of zinc at the negative electrode makes the mid-overpotential during the charging process higher than that during the discharging process at 0 °C. However, the mid-overpotentials of the positive electrode during the charging process are much larger than that during the discharging process. This is due to the different activity caused by the different transfer coefficient. The anodic current (i_a) and cathodic current (i_c) are expressed as follows:

$$i_a = nFAk^0 C_R(0,t)e^{-\alpha f(E-E^{\theta\prime})}$$

$$i_c = nFAk^0 C_O(0,t)e^{\beta f(E-E^{\theta\prime})}$$

where n is the electron transfer number, F is the Faradic constant, A is the electrode surface, k^0 is the rate constant of kinetic reaction, $C_O(0,t)$ and $C_R(0,t)$ are the concentrations of the reactants at the electrode surface, α and β are the mass transfer coefficient during redox processes, which reflects the effect of activation energy on the overpotential, f is the constant, E is the reacted potential, $E^{\theta\prime}$ is the equilibrium potential. It is obvious that the $C_O(0,t)$ and $C_R(0,t)$ are equal at the mid-time for both charging and

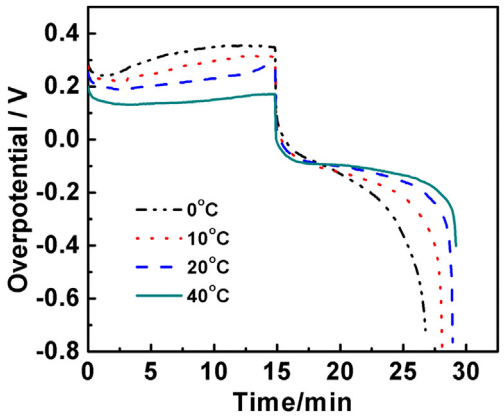

Fig. 6. Overpotential of positive electrode under various temperatures.

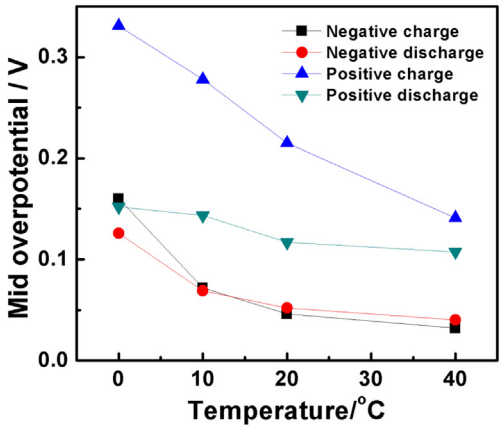

Fig. 8. Mid-overpotential under various temperatures.

discharging process. In this study, the absolute value of i_a and i_c are controlled to be equal during the charging and discharging process. Accordingly, the ratio of anodic overpotential to cathodic overpotential is equal to β/α. This is the reason that the charge overpotential is larger than discharge overpotential on the positive electrode.

The mid-overpotential of the positive electrode during the charging process is the most sensitive to temperature than that during the positive discharging, negative charging and negative discharging processes. During the positive charging process, a proton, diffusing from the solid material to the solid/electrolyte interface, reacts with a hydroxyl ion to form water, and an electron flow from the conducting substrate to the external electric circuit. It is well-known that the charging reaction rate of the positive electrode ($Ni(OH)_2 - e \rightarrow NiOOH + H^+$) is determined by the proton transfer rate in solid active material [22,24,25]. Accordingly, the temperature has a remarkable influence on the proton transfer rate. In short, the positive polarization is the dominant contributor during both charging and discharging processes. Urgent needs are also in the fabrication of highly active nickel hydroxide electrode consisting of rapid ion, proton and electron transport pathways.

4. Conclusions

Our extensive study on the temperature effect on ZNBs and in situ polarization analysis shows: i) no obstacle was observed in start-up at all temperatures (from 0 °C to 40 °C), ii) ZNBs can operate at a wide temperature range with acceptable energy efficiency (53%–79.1%), iii) the temperature sensitivity of CE and EE are 0.65% $°C^{-1}$ and 0.98% $°C^{-1}$, respectively, iv) the positive polarization accounts for the major part of full-cell polarization, v) the proton transfer in positive electrode is more sensitive to temperature. All above results reveal that ZNBs possess extensive application prospect with well temperature adaptability. These results point out the struggling direction to further improve the battery performance, which thereby promotes the commercial applications.

Acknowledgment

This work is financially supported by the National Basic Research Program of China (973 Program No. 2010CB227204).

References

[1] C. Ponce de León, A. Frías-Ferrer, J. González-García, D.A. Szánto, F.C. Walsh, J. Power Sources 160 (2006) 716–732.
[2] M. Skyllas-Kazacos, M.H. Chakrabarti, S.A. Hajimolana, F.S. Mjalli, M. Saleem, J. Electrochem. Soc. 158 (2011) R55.
[3] W. Wei, H. Zhang, X. Li, H. Zhang, Y. Li, I. Vankelecom, PCCP 15 (2013) 1766–1771.
[4] H. Zhang, H. Zhang, X. Li, Z. Mai, W. Wei, Energy Environ. Sci. 5 (2012) 6299.
[5] M. Vijayakumar, B. Schwenzer, S. Kim, Z.G. Yang, S. Thevuthasan, J. Liu, G.L. Graff, J.Z. Hu, Solid State Nucl. Magn. Reson. 42 (2012) 71–80.
[6] S.-G. Park, N.-S. Kwak, C.W. Hwang, H.-M. Park, T.S. Hwang, J. Membr. Sci. 423–424 (2012) 429–437.
[7] S.-J. Seo, B.-C. Kim, K.-W. Sung, J. Shim, J.-D. Jeon, K.-H. Shin, S.-H. Shin, S.-H. Yun, J.-Y. Lee, S.-H. Moon, J. Membr. Sci. 428 (2013) 17–23.
[8] J. Qiu, M. Zhai, J. Chen, Y. Wang, J. Peng, L. Xu, J. Li, G. Wei, J. Membr. Sci. 342 (2009) 215–220.
[9] A. Hazza, D. Pletcher, R. Wills, PCCP 6 (2004) 1773–1778.
[10] Y. Zhao, S. Si, C. Liao, J. Power Sources 241 (2013) 449–453.
[11] P.K. Leung, C. Ponce de León, F.C. Walsh, Electrochem. Commun. 13 (2011) 770–773.
[12] Q. Lai, H. Zhang, X. Li, L. Zhang, Y. Cheng, J. Power Sources 235 (2013) 1–4.
[13] Y. Wen, T. Wang, J. Cheng, J. Pan, G. Cao, Y. Yang, Electrochim. Acta 59 (2012) 64–68.
[14] Y. Ito, X. Wei, D. Desai, D. Steingart, S. Banerjee, J. Power Sources 211 (2012) 119–128.
[15] Y. Cheng, H. Zhang, Q. Lai, X. Li, D. Shi, Electrochim. Acta 105 (2013) 618–621.
[16] Y. Cheng, H. Zhang, Q. Lai, X. Li, D. Shi, L. Zhang, J. Power Sources 241 (2013) 196–202.
[17] M. SkyllasKazacos, C. Menictas, M. Kazacos, J. Electrochem. Soc. 143 (1996) L86–L88.
[18] M. Kazacos, M. Cheng, M. Skyllas-Kazacos, J. Appl. Electrochem. 20 (1990) 463–467.
[19] X. Li, D. Pletcher, F.C. Walsh, Electrochim. Acta 54 (2009) 4688–4695.
[20] V.S. Bagotsky, Fundamentals of Electrochemistry, second edn., Wiley, 2006, p. 193.
[21] M. Paunovic, M. Schlesinger, Fundamentals of Electrochemical Deposition, second edn., Wiley-Interscience, New Jersey, 2006.
[22] S. Motupally, J. Electrochem. Soc. 145 (1998) 29.
[23] J.W. Weidner, J. Electrochem. Soc. 141 (1994) 346.
[24] D.M. MacArthur, J. Electrochem. Soc. 117 (1970) 729.
[25] C. Zhang, S.-M. Park, J. Electrochem. Soc. 134 (1987) 2966–2970.